Development of a novel, highly quantitative in vivo model for the study of biofilm-impaired cutaneous wound healing

Anandev N. Gurjala, MD, MS[1]; Matthew R. Geringer, BS[1]; Akhil K. Seth, MD[1]; Seok J. Hong, PhD[1]; Mark S. Smeltzer, PhD[2]; Robert D. Galiano, MD[1]; Kai P. Leung, PhD[3]; Thomas A. Mustoe, MD[1]

1. Division of Plastic Surgery, Feinberg School of Medicine, Northwestern University, Chicago, Illinois,
2. Department of Microbiology and Immunology, University of Arkansas Medical Sciences, Little Rock, Arkansas, and
3. Microbiology Branch, US Army Dental and Trauma Research Detachment, Institute of Surgical Research, Fort Sam Houston, Texas

Reprint requests:
Thomas A. Mustoe, Division of Plastic Surgery, Feinberg School of Medicine, Northwestern University, 675 N. St. Clair, Suite 19 250, Chicago, IL 60611.
Tel: +1 312 695 6022;
Fax: +1 312 695 5672;
Email: tmustoe@nmh.org

Manuscript received: September 24, 2010
Accepted in final form: January 25, 2011

DOI:10.1111/j.1524 475X.2011.00690.x

ABSTRACT

A growing body of evidence suggests that in addition to hypoxia, ischemia-reperfusion injury, and intrinsic host factors, bacterial biofilms represent a fourth major pillar in chronic wound pathogenesis. Given that most studies to date rely on in vitro or observational clinical data, our aim was to develop a novel, quantitative animal model enabling further investigation of the biofilm hypothesis in vivo. Dermal punch wounds were created in New Zealand rabbit ears, and used as uninfected controls, or inoculated with green fluorescent protein-labeled *Staphylococcus aureus* to form wounds with bacteria predominantly in the planktonic or biofilm phase. Epifluorescence and scanning electron microscopy revealed that *S. aureus* rapidly forms mature biofilm in wounds within 24 hours of inoculation, with persistence of biofilm viability over time seen through serial bacterial count measurement and laser scanning confocal imaging at different time points postwounding and inoculation. Inflammatory markers confirmed that the biofilm phenotype creates a characteristic, sustained, low-grade inflammatory response, and that over time biofilm impairs epithelial migration and granulation tissue in-growth, as shown histologically. We have established and validated a highly quantitative, reproducible in vivo biofilm model, while providing evidence that the biofilm phenotype specifically contributes to profound cutaneous wound healing impairment. Our model highlights the importance of bacterial biofilms in chronic wound pathogenesis, providing an in vivo platform for further inquiry into the basic biology of bacterial biofilm–host interaction and high-throughput testing of antibiofilm therapeutics.

Bacterial biofilms, sessile communities of bacteria encased in a protective polysaccharide matrix, can find harbor in many parts of the body, having been reported on biological surfaces as disparate as myocardium, nasal epithelium, and dental enamel.[1] On each of these surfaces the relationship between bacteria and host may range from purely commensal (as in the intestinal gut) to highly destructive when established on microbiologically naive tissues (such as in endocarditis or cystic fibrosis). Whether on damaged heart valves or poorly functioning respiratory epithelium, the pathophysiology of bacterial biofilms remains conserved: host defenses are rendered unable to clear biofilm due to its adaptive survival mechanisms, and yet are constantly stimulated by its physical presence, shedding of planktonic bacteria, and elaboration of virulence factors. The result is a chronic inflammatory cycle causing injury to host tissues over time.[2]

In recent years the wound bed of compromised skin has been thought to offer yet another biological surface onto which bacterial biofilms can take hold. The susceptibility of open wounds to bacterial seeding and the moist, nutritionally supportive microenvironment of the wound matrix create an ideal setting for biofilm to interfere with the wound healing process. Phil Stewart from Montana State University in particular has put forth a considerable series of papers articulating this hypothesis. In a clinical study of human wounds, his group convincingly demonstrated using light and scanning electron microscopy (SEM) that bacteria in biofilm-phase are present in all types of chronic wounds, establishing a key link between biofilm and nonhealing.[3] Studies by other groups using sophisticated molecular techniques for bacterial recovery have further established that a diverse array of bacterial species exists in human chronic wounds, and that these bacteria persist over time.[4,5] Moreover, a variety of in vitro models have made essential contributions, including demonstration of robust biofilm resistance to antimicrobials,[6] important genetic pathways for bacterial communication including quorum sensing,[7] and even inhibitory effects of biofilms against cultured human keratinocytes.[8]

While the aforementioned studies have been crucial to developing an understanding of biofilm in wounds, equivalent strides have not been made in the area of in vivo experimentation, principally due to the lack of an established animal model. Given the complexity of wound healing, extrapolation from in vitro biofilm studies to the clinic has

Report Documentation Page

Form Approved
OMB No. 0704-0188

1. REPORT DATE	2. REPORT TYPE	3. DATES COVERED
01 MAY 2011	**N/A**	**-**

4. TITLE AND SUBTITLE	5a. CONTRACT NUMBER
Development of a novel, highly quantitative in vivo model for the study of biofilm-impaired cutaneous wound healing.	5b. GRANT NUMBER
	5c. PROGRAM ELEMENT NUMBER
6. AUTHOR(S)	5d. PROJECT NUMBER
Gurjala A., Geringer M. R., Hong S.-J. Smeltzer M. S., Galiano R. D., Leung K. P., Mustoe T. A.,	5e. TASK NUMBER
	5f. WORK UNIT NUMBER
7. PERFORMING ORGANIZATION NAME(S) AND ADDRESS(ES) **United States Army Institute of Surgical Research, JBSA Fort Sam Houston, TX**	8. PERFORMING ORGANIZATION REPORT NUMBER
9. SPONSORING/MONITORING AGENCY NAME(S) AND ADDRESS(ES)	10. SPONSOR/MONITOR'S ACRONYM(S)
	11. SPONSOR/MONITOR'S REPORT NUMBER(S)

12. DISTRIBUTION/AVAILABILITY STATEMENT
Approved for public release, distribution unlimited

13. SUPPLEMENTARY NOTES

14. ABSTRACT

15. SUBJECT TERMS

16. SECURITY CLASSIFICATION OF:			17. LIMITATION OF ABSTRACT	18. NUMBER OF PAGES	19a. NAME OF RESPONSIBLE PERSON
a REPORT	b ABSTRACT	c THIS PAGE			
unclassified	**unclassified**	**unclassified**	**UU**	**11**	

been challenging, because only animal models can take into account such critical in vivo factors as the interplay of the host immune response and wound bed components with bacteria. Secondly, human studies have been only observational and correlative, lacking the experimental and causative data necessary to fully establish the biofilm hypothesis. There is thus a wide consensus among the biofilm research community on a need for more in vivo biofilm models, and that they will be necessary tools for furthering our understanding of biofilm–host biology.

In the present study we aim to build on previous work by developing a novel, in vivo biofilm model in rabbit, capable of precisely defining the impact of biofilms on cutaneous wound healing. Through rigorous testing, we validate that our model allows for biofilm formation within wounds and maintenance of its structure and viability over time. Although wound infections represent a spectrum of bacterial phenotypes, involving bacteria in both the planktonic and biofilm phases, we use our model to study differences in planktonic- and biofilm-dominant infections, which are classically associated with acute and chronic wound pathogenesis, respectively. In particular, we hypothesize that both planktonic-dominant, or active, and biofilm-dominant wound infections will show severe wound healing deficits when compared with uninfected wound beds. Furthermore, we propose that phenotypic differences between these two types of infection will lead to distinct host inflammatory responses even under circumstances where both infections have similar bacterial burdens. Through these experiments, we hope to further define the intricacies of wound bacterial biofilms, while introducing and establishing an in vivo biofilm model that will serve as a foundation for further mechanistic and clinically relevant investigation.

MATERIALS AND METHODS

Animals

Young, adult New Zealand white rabbits (3–6 months, $\sim$3 kg) were acclimated to standard housing and fed ad libitum under a protocol approved by the Animal Care and Use Committee at Northwestern University. All animals were housed in individual cages under constant temperature (22 °C) and humidity with a 12-hour light–dark cycle. A total of 82 rabbits were used in the development of this model after a series of pilot studies manipulating the following variables in different permutations: wound size, wound location, number of wounds per ear, wound depth (partial vs. full thickness), timing of inoculation, length of antibiotic treatment, type of absorptive dressing, timing of dressing changes, and length of wound healing period before harvest. Following exhaustive characterization of these permutations the final model protocol described below was chosen based on recapitulation of essential aspects of the human biofilm-infected chronic wound.

Bacterial strains, plasmid, and phage transduction

Staphylococcus aureus strain UAMS-1[9,10] was grown on tryptic soy agar (TSA) and in tryptic soy broth (TSB) at 37 °C. The green fluorescent protein (GFP)-expressing plasmid, pCN57, was introduced to UAMS-1 by phage transduction as described by Charpentier et al.[11] with modifications. Briefly, strain RN9623 (recently designated as NARSA strain ID# NRS623, which contains pCN57) was cultured to exponential growth phase in TSB containing 5 mM $CaCl_2$ (Sigma-Aldrich, St. Louis, MO) and 10 μg/mL erythromycin (Sigma-Aldrich). To prepare phage lysates, strain RN9623 was infected with phage 11 at a multiplicity of infection (MOI) 0.5 and cultured at 37 °C until cell lysis occurred. Lysates were centrifuged to remove cell debris and filtered through a 0.45 μm filter. For transduction, phage lysates at a MOI 0.2 were incubated with UAMS-1 that has been resuspended in TSB containing 5 mM $CaCl_2$. After 20 minutes incubation at 37 °C, the reaction mixture was washed with ice-cold 20 mM sodium citrate and plated in TSA containing 10 μg/mL erythromycin. The presence of pCN57 in UAMS-1 was confirmed by plasmid isolation, restriction analysis, and fluorescence microscopy.

Wound protocol and bacteria biofilm model

For creation of the dermal wounds, the rabbits were anesthetized with an intramuscular injection of ketamine (22.5 mg/kg) and xylazine (3.5 mg/kg) mixture before surgery. Ears were shaved and sterilized with a betadine scrub and 70% ethanol. Following intradermal injection of 1% lidocaine with epinephrine local anesthetic, six 6-mm-diameter full-thickness dermal wounds were created down to the perichondrium on the ventral surface of the ear and dressed with semiocclusive transparent film (Tegaderm®, 3M Health Care, St. Paul, MN). For the control arm of the experiments, wounds were redressed with sterile Tegaderm® on postoperative days (PODs) 3, 5, 6, 8, and 10. For the infected wound groups, bacteria grown on agar plates were harvested and proliferated in culture medium broth, followed by suspension in phosphate buffer solution (PBS), from which a concentration was measured. Approximately 10^6 colony-forming units (CFUs) of planktonic bacteria were inoculated from suspension onto each wound bed on POD 3 and allowed to proliferate under the Tegaderm® dressing. For the active infection arm, planktonic bacteria were allowed to continue active proliferation, with Tegaderm® dressing changes on PODs 5, 6, 8 and 10. For the biofilm arm, topical mupirocin (2%) antibiotic ointment (Teva Pharmaceuticals, Sellersville, PA) was applied on POD 4 to eliminate planktonic-phase bacteria and create a predominantly biofilm-phase infection. In order to prevent seroma formation and maintain biofilm-phase infection by preventing regrowth of planktonic bacteria, an antimicrobial absorbent dressing containing polyhexamethylene biguanide (Telfa® AMD, Tyco Healthcare Group, Mansfield, MA) was applied to biofilm wounds on PODs 5, 6, 8, and 10. All dressings were checked daily throughout the entire protocol.

Harvesting of wounds

After euthanizing the animals by an intracardiac euthasol injection, wounds were harvested for various analyses. For the biofilm time course experiment, wounds were harvested at 6-hour intervals following inoculation until 24 hours, and analyzed by epifluorescence and SEM. To test

for the presence of bacteria in the wound bed, bacterial counts and laser scanning confocal microscopy were conducted on PODs 4, 6, 8, 10, and 12. In addition, SEM was performed POD 12 to visually confirm biofilm formation within the wound bed. For the wound healing experiments, wounds were harvested at POD 12 for histological analysis using hematoxylin & eosin (H&E) staining. RNA extraction and reverse transcription quantitative polymerase chain reaction (qPCR) was carried out on POD 6 and POD 12 on wounds to determine the cytokine profiles as the result of the host inflammatory response.

Viable bacterial counts using drop plate method

For viable bacterial counts, wound beds were biopsied with 10 mm punches and using No. 15 scalpels (Becton Dickinson AcuteCare, Franklin Lakes, NJ) the wound beds were excised and tissue samples collected into separate MagNA Lyser Green Beads tubes (Roche Diagnostics, Indianapolis, IN) each containing 1 mL of PBS. All samples were homogenized at 5,000 rpm for 30 seconds (MagNA Lyser, Roche Diagnostics), and then sonicated (Microson Ultrasonic Cell Disrupter, Heat Systems-Ultrasonics Inc., Farmingdale, NY) for 2 minutes at 5–8 W to break up any bacterial aggregates that were present in wound samples. Time interval and power setting used for the sonication were preempirically determined to ensure that bacterial viability was maintained in the process.

The resulting solutions were serially diluted and plated on both Blood Agar (Hardy Diagnostics, Santa Maria, CA) and Lipovitellin Salt Mannitol Agar (selective medium for *S. aureus*) (Hardy Diagnostics) and incubated overnight at 37 °C. CFUs were determined by the standard colony counting method.

Histological analysis

Wounds were excised with a 10 mm punch and bisected at their largest diameter for H&E staining. Tissues were fixed in formalin, embedded in paraffin, cut into 4 μm sections, and stained to be analyzed under a light microscope. Slides were examined for quantification of epithelial and granulation gap, and total granulation area using a digital analysis system (NIS-Elements Basic Research, Nikon Instech Co., Kanagawa, Japan) as described previously.[12] Two blinded and independent observers evaluated all histological sections. The results of both examiners were averaged. Slides were omitted if results differed $> 30\%$ among examiners.

Fluorescent staining and laser scanning confocal microscopy

Wound samples for fluorescence staining were embedded in O.C.T. Compound (Sakura Finetek, Torrance, CA), snap-frozen in liquid nitrogen, and stored at −80 °C until time of cryosectioning. Ten micrometer sections of biofilm-infected wound tissues were prepared with the use of a cryostat. Sections for the biofilm time course experiment were stained with concanavalin-A conjugated to Texas Red (Invitrogen, Carlsbad, CA) to identify the presence of exopolysaccharides rich in mannose and glucose that are commonly the basis of biofilm extracellular matrix (ECM), and with 4′-6-diamidino-2-phenylindole to visualize host cells. Section slides were also analyzed using laser scanning confocal microscopy (Zeiss LSM 510 META, Carl Zeiss Microimaging, LLC, Thornwood, NY) to visualize GFP-labeled *S. aureus*.

SEM

To determine the structure of biofilms formed in rabbit ear wounds, wound samples were mounted by double-sided tape to specimen stubs, and examined "in situ" by variable pressure SEM. The procedure bypasses the steps for sample preparation used in conventional SEM and therefore minimizes the introduction of artifacts, providing an excellent preservation of sample integrity. Imaging of the samples was accomplished by the use of a Carl Zeiss 1450 VP scanning electron microscope (Carl Zeiss Microimaging, LLC) operated at the gas chamber pressure of 70 Pa with the specimen cooling stage set at −25 °C and the scanning voltage set at 10 kV.

Total mRNA extraction and reverse-transcription qPCR

Wounds were harvested for mRNA extraction and subsequent cDNA conversion as part of reverse transcription qPCR. The dermal layer on the ventral side of the ear was removed and the wound bed and circumferential areas (rings) extending from the wound bed were punched out and immediately snap-frozen in liquid nitrogen. Wound samples were homogenized using a Mini-bead beater-8 equipment (Biospec Products Inc., Bartlesville, OK) using zirconia beads (2.0 mm diameter, Biospec Products Inc.) in the presence of Trizol Reagent (Sigma-Aldrich). Total RNA was isolated according to the manufacturer's protocol. Contaminating genomic DNA during RNA preparation was removed using the Turbo DNA-free kit (Ambion, Austin, TX). Five μg of total RNA was used to prepare cDNA using superscript II (Invitrogen) with 100 ng of random primers (Invitrogen).

For quantitative analysis of the expression level of mRNAs, real time qPCR analyses using SYBR green 1 were performed utilizing an ABI prism 7000 sequence detection system (Applied Biosystems, Foster City, CA). PCR primers were designed using the Primer 3 program (http://frodo.wi.mit.edu/). Expression of each gene was normalized to the level of glyceraldehyde 3-phosphate dehydrogenase (GADPH), the house keeping gene, to get ΔC_t. The $2^{\Delta\Delta C_t}$ method was used to calculate gene expression of interleukin (IL)-1β and tumor necrosis factor-α (TNF-α) of control, biofilm-infected wounds, and wounds under active infection. Expression of genes was detected by PCR with the following oligonucleotides: IL-1β (5′-CCACAGTGGCAATGAAAATG-3′ and 5′-AGAAAGTTCTCAGGCCGTCA-3′), TNF-α (5′-CCAGATGGTCACCCTCAGAT-3′ and 5′-TGTTCTGAGAGGCGTGATTG-3′), GADPH (5′-AGGTCATCCACGACCACTTC-3′ and 5′-GTGAGTTTCCCGTTCAGCTC-3′).

Statistical analysis

Data are presented in graphical form as mean ± standard errors and were analyzed using the Student's *t*-test (two-tailed and unpaired) to compare controls, active infection, and biofilm wound samples. The level of significance was set at $p < 0.05$.

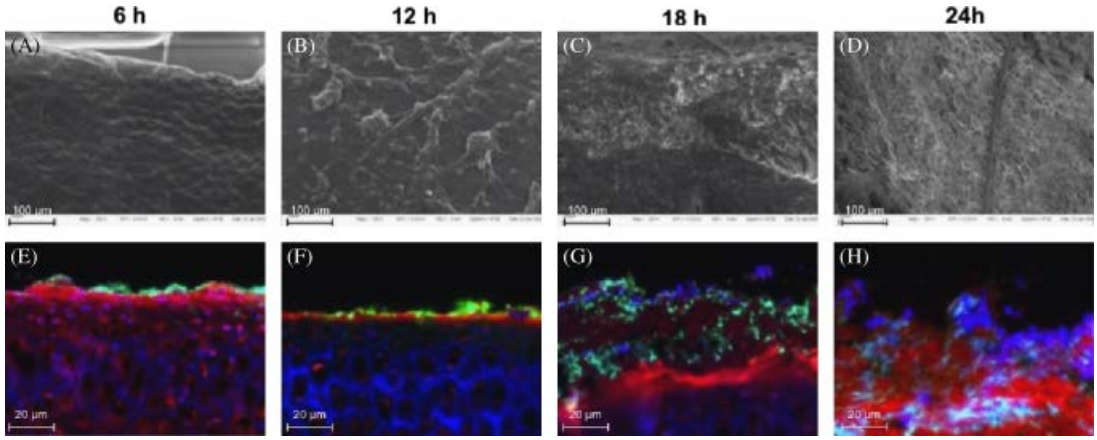

Figure 1. Time-course of biofilm development in 6-hour intervals from inoculation to the formation of mature biofilm. *Staphylococcus aureus* establishes a mature biofilm in rabbit dermal ulcers within 24 hours as reviewed by scanning electron microscopy (SEM) (A–D) and fluorescence light microscopy (E–H). (A) and (E) show that at 6 hours postinfection bacteria (green) sparsely cover the wound surface (blue). At 12 hours postinfection *S. aureus* spreads more evenly over the wound surface (B and F). (C) and (G) show that by 18 hours postinfection *S. aureus* assumes early biofilm morphology. Note the change of architecture of the biofilm as revealed by SEM. By 24 hours postinfection, a mature biofilm of *S. aureus* is formed with bacteria encased within exopolysaccharide matrix (red) (D and H) (magnification: A–D, ×200; E–H, ×1,000).

RESULTS

To determine the kinetics of biofilm formation in vivo, a time-course study using the rabbit biofilm wound model was performed. The results showed that *S. aureus* formed a mature biofilm within 24 hours in wounds after inoculation (Figure 1). A spatially organized three-dimensional biofilm structure began to emerge 18 hours postinoculation as revealed by SEM (Figure 1C). At 24 hours postinoculation the bacteria on the wound became more organized showing a complex architecture with dense ECM (Figure 1D). Staining of mannose and glucose moieties within the wound by Texas Red-labeled concanavalin A also revealed increasing exopolysaccharides around the bacteria such that by 24 hours they are completely encased by a carbohydrate-rich ECM as shown by epifluorescence microscopy (Figure 1G and H).

As part of model testing and validation, biofilm development and viability was verified through several different techniques. Viable bacterial counts, measured at multiple time points following inoculation, showed the persistence of live bacteria within the wound beds of biofilm animals (Figure 2). In particular, following inoculation on POD 3 with approximately 10^6 CFUs of planktonic bacteria, an initial proliferation on POD 4 up to 10^7 is followed by topical antibiotic and absorptive, antimicrobial dressing placement, resulting in a significant ($p < 0.05$) decreased number of viable bacteria at POD 6. This decrease can be attributed to the elimination of free-floating planktonic bacteria, creating a biofilm-dominant wound. However, between POD 6 and POD 12, biofilm wounds maintain a consistent level of viable bacteria averaging between 10^5 and 10^6 CFUs per infected wound, verifying that wounds maintain live biofilm bacteria throughout the time-course of our animal model. This consistency models the presumed ''steady-state'' that develops between chronic wound biofilms and their respective hosts. To correlate with bacterial count measurements, laser scanning confocal microscopy was also performed at these time points, showing the presence of GFP-labeled *S. aureus* at POD 6 (Figure 3A) and POD 12 (Figure 3B) within the wound bed, clearly separated from the underlying, intact ear cartilage. In addition, SEM was performed at POD 12, showing the presence of individual bacteria within a well

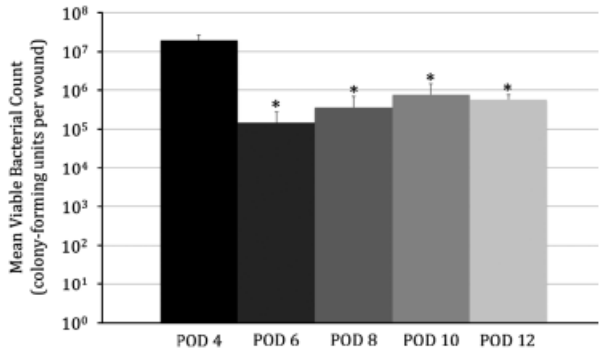

Figure 2. Viable bacterial count measurements from biofilm-infected wounds at successive time points following inoculation on POD 3. Inoculation with approximately 10^6 colony-forming units (CFUs) of *Staphylococcus aureus* is followed by an initial proliferation of bacteria by POD 4, followed by topical antibiotic and antimicrobial, absorbent gauze placement to develop and maintain a biofilm-dominant wound. Note an initial significant decrease in viable bacteria between POD 4 and POD 6, most likely representing the elimination of free-floating planktonic bacteria by the aforementioned treatment methods. Successive bacterial count measurement at PODs 6, 8, 10, and 12 show viable bacteria that are maintained at a consistent level over time, averaging between 10^5 and 10^6 CFUs per wound, representative of the ''steady-state'' that is often seen between wound biofilms and their respective hosts (*$p < 0.05$) (n=8–15 wounds/time-point). POD, postoperative day. Error bars signify standard error of means.

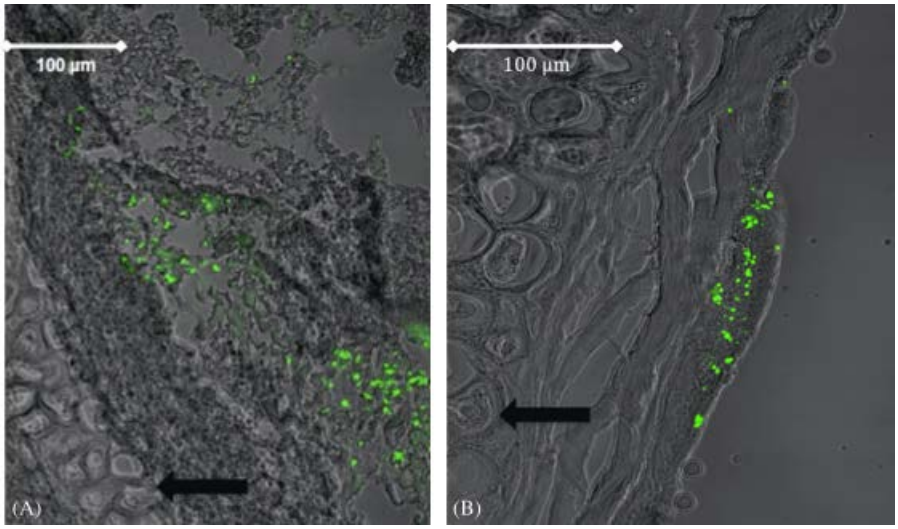

Figure 3. Laser scanning confocal microscopy of biofilm wounds infected with green fluorescent protein-labeled *Staphylococcus aureus*. Imaging done at POD 6 and POD 12 validates the presence of viable bacteria within biofilm wounds over the course of time used in our model. Note the clustering of bacteria within the wound bed (green) with underlying intact cartilage of the ear (arrow) (magnification×20). POD, postoperative day.

developed, encasing biofilm matrix architecture that covered the wound bed surface (Figure 4)

Despite the spectrum of infection that exists between planktonic- and biofilm-phase bacteria, our model has been developed to create a distinct infection phenotype characterized by a predominance of biofilm-phase bacteria. To show this model capability, viable bacterial counts were performed from biofilm-dominant and planktonic-dominant, i.e., active infection, wounds at POD 6 (Figure 5A). This analysis revealed no significant difference in viable bacteria despite differences in how the wounds were treated. At this same time-point, host inflammatory response to these two types of infections was quantified using real-time qPCR (Figure 5B and C). Biofilm infection elicited a significantly lower-grade host response ($p < 0.05$), measured through IL-1β and TNF-α expression, than active infection wounds, indicating a true phenotypic difference in the bacteria–host response between these two types of infection despite a similar bacterial burden. In addition, when the expression of these inflammatory mediators in biofilm wounds was measured at POD 12, there is evidence of a maintained low-grade host response, with minimal decrease in the level of TNF-α expression and a continued high level of IL-1β expression. (Figure 6) To ensure that our model created only localized wound infections, thus preventing the activation and influence of systemic inflammatory mediators, successively larger circumferential rings of tissue were analyzed outside of the wound bed. As seen in Figure 7, expression of inflammatory mediators quickly tapers to significantly lower levels in both biofilm and active infection wounds ($p < 0.05$), verifying that our model maintains a localized wound infection. Furthermore, no animals in either group showed signs of systemic infection and maintained normal body weights throughout the experimental period (data not shown). These data not only distinguish and characterize the biofilm wound phenotype, which triggers and maintains a low-grade host inflammatory response, but also validate the sensitivity of our model to distinguish

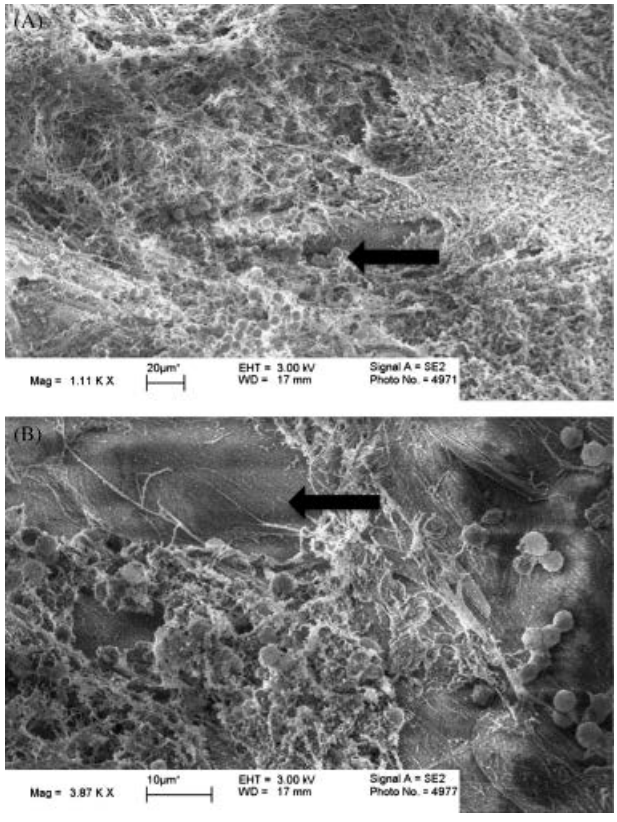

Figure 4. Scanning electron microscopy of *Staphylococcus aureus* biofilm-infected wounds on POD 12 showing developed biofilm architecture. (A) Intricate extracellular matrix encases individual bacterial cells (arrow) in dense, lattice-like structure (magnification ∼×1000). (B) Higher magnification view of individual *S. aureus* with surrounding extracellular matrix material adjacent to bare wound surface (arrow) (magnification ∼× 4000). POD, postoperative day.

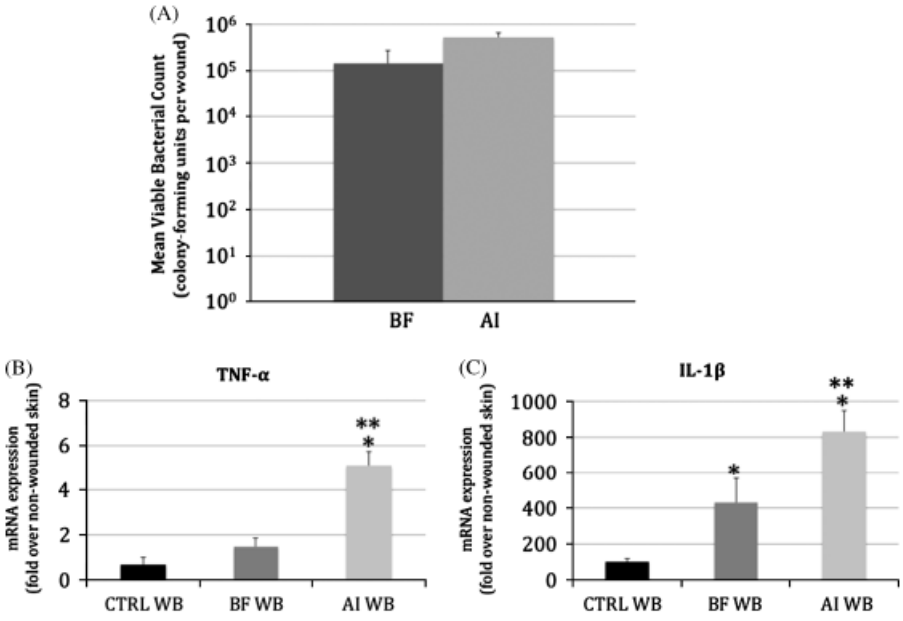

Figure 5. Demonstration of phenotypic differences between biofilm- and planktonic-dominant (i.e., active infection) wounds. (A) At POD 6, there is no significant difference in viable bacterial counts between untreated active infection (AI) wounds and treated biofilm-dominant (BF) wounds (n=15 wounds/group). (B) and (C) despite similar bacterial burdens, biofilm wounds trigger a significantly lower-grade host inflammatory response, measured through interleukin (IL)-1β and tumor necrosis factor-α (TNF-α) wound bed (WB) expression, as compared with active infection wounds. This validates a phenotypic difference between the two infection groups in their interaction with the host (*$p < 0.05$ as compared with CTRL; **$p < 0.05$ as compared with BF) (n=6 wounds/group). POD, postoperative day. Error bars signify standard error of means.

between these different wound phenotypes despite similar levels of initial bacterial burden.

Having established and validated our wound biofilm model, we aimed to assess the effects of *S. aureus* biofilm on quantitative wound healing parameters histologically. Wounds were harvested on POD 12, with gross evidence of minimal wound healing in both biofilm- and planktonic-dominant (active infection) wounds as compared with control (Figure 8). Also note the increased level of purulent exudate over active infection wounds (Figure 8B) as compared with the so-called "film" overlying biofilm wounds (Figure 8C), consistent with the differences seen in host inflammatory response. Looking histologically, *S. aureus* in the form of active or biofilm infections impaired cutaneous wound healing (Figure 9). Infected wounds showed delayed reepithelialization over the wound bed and thickening of the epidermal layer at the leading edge (Figure 9B and C). Differences between active infection and biofilm are also seen in the cartilage and debris around the wound bed. In the active infection, highly virulent and invasive planktonic bacteria damage the cartilage, while biofilm histology shows cartilage integrity. Large amounts of debris in the active infection were present representing an increased influx of white blood cells (neutrophils) above the wound bed. The debris was also found in the biofilm, but significantly reduced, confirming a decreased inflammatory response histologically. Through quantitative image analysis, measurement of epithelial gap (Figure 10A), granulation tissue gap (Figure 10B), and new granulation tissue (Figure 10C) showed significant differences across all analyzed parameters between control and infected groups ($p < 0.05$), verifying that our model is capable of simulating the impairment of wound-healing seen in biofilm-infected wounds.

DISCUSSION

Predating any bacterial biofilm theories, chronic wounds of all types have shared a common characteristic: a persistent inflammatory state, marked by a destructive milieu

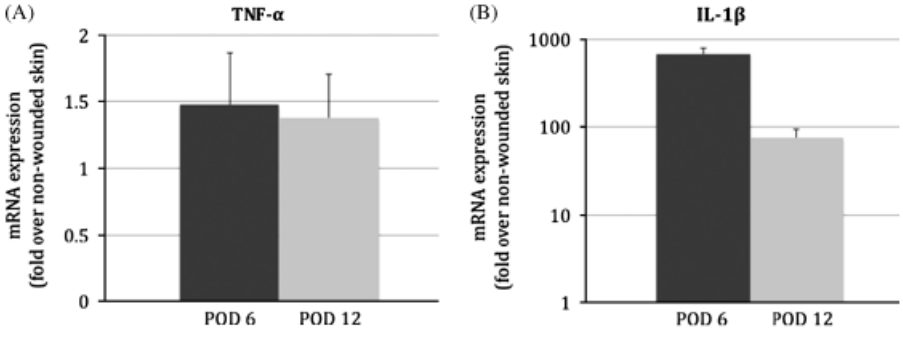

Figure 6. Maintenance of a low-grade inflammatory response secondary to biofilm wound infection over time. (A) Expression of tumor necrosis factor-α (TNF-α) is maintained between POD 6 and POD 12 at very similar levels. (B) Interleukin (IL)-1β expression is decreased but remains markedly elevated at POD 12, validating the idea that biofilm triggers a low-grade, chronic inflammatory response, which can be simulated through this model (n=6 wounds/group). POD, postoperative day. Error bars signify standard error of means.

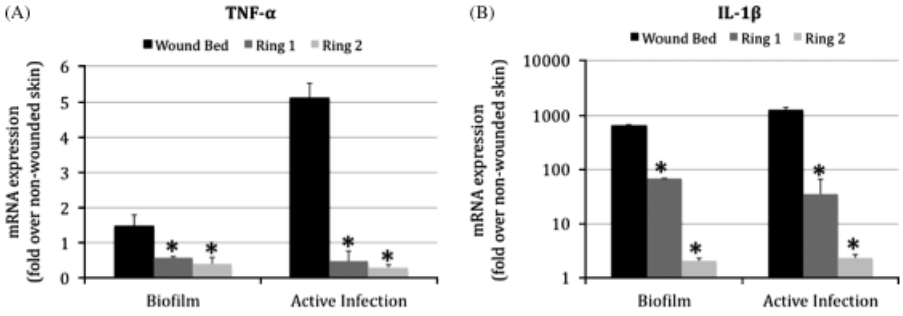

Figure 7. Comparison of inflammatory profiles from control and infected wounds, showing highly localized infections at POD 6. Note significantly higher level of inflammatory mediator expression for both tumor necrosis factor-α (TNF-α) (A) and interleukin (IL)-1β (B) within wound beds of infected wounds as compared with successive outer rings (ring 1: concentric ring of tissue 2 mm distal to the wound edge; ring 2: concentric ring of tissue 2 mm distal to the edge of ring 1) (*$p < 0.05$ as compared with wound bed) (n=6 wounds/group). POD, postoperative day. Error bars signify standard error of means.

and failure of the wounds to progress normally into the proliferative and remodeling phases of wound healing.[13] Clinically, chronic wounds are observed to languish in a friable, highly exudative, and oftentimes ''slimy'' condition, most displaying no evidence of planktonic or frankly purulent bacterial infection, some responding to frequent debridement and wound care, and others remaining recalcitrant to wound healing interventions.[14]

Bacterial biofilms offer a powerful and parsimonious explanation for both the cause and persistence of the inflammatory arrest of chronic wounds. The logical connection between bacteria and chronic wounds is intuitively clear, but was likely delayed by medicine's historic reliance on planktonic culture techniques, which fail to recover biofilm phase bacteria, especially from chronic wound samples. Indeed, as biofilms have recently been found using more sophisticated techniques to be present in pressure sores, venous stasis ulcers, and diabetic foot ulcers—traditionally regarded as having distinct etiologies—all three chronic wound archetypes may in fact be linked by a single contributing factor. This factor has high potential as a therapeutic target, as elimination of bacterial biofilms alone could be instrumental in shifting the balance between inhibitory and vulnerary factors toward a healing phenotype. In addition to the classic tenets of hypoxia, ischemia-reperfusion, and intrinsic host disease, then, bacterial biofilms hold considerable promise as a fourth major pillar of impaired wound healing.[15]

The addition of biofilm theory to wounds has increased our understanding of bacteria–host interaction. Whereas wound microbiology was conventionally conceptualized as contamination, colonization, and infection by planktonic bacteria, it is now clear that biofilm phase bacteria play a prominent role in the spectrum of clinical wounds.[16] This spectrum includes both infections that are predominantly in the planktonic- or biofilm-phases, although it is clear that a mixture of bacterial phenotypes can, and tend to, exist within a given wound. There is likely a balance between host vulnerary factors/defenses and bacterial proliferation in its various forms, the predominance of which influences wound outcome. Bacteria in a wound may be either overcome or cleared by host defenses; if bacteria persist as biofilms, they may be held in check by the host defenses, yet create a state of chronic low-grade inflammation. Given this expanded view of wound microbiology, it is critical that any in vivo model of biofilm simulate both its ability to impair cutaneous wound healing and its maintenance of a low-grade, chronic inflammatory host response that is distinct from the response to a more ''active'' planktonic-dominant infection.

Recent work has taken important steps toward achieving an in vivo biofilm model, with Rashid et al.[17] showing that cutaneous *Pseudomonas aeruginosa* biofilm can be experimentally grown in thermally induced mouse wounds. Using their porcine model, Davis and colleagues inoculated *S. aureus* onto partial thickness cutaneous wounds, and assessed for presence of biofilm after 48 hours. Multiple modes of imaging were able to confirm presence of living biofilm in these wounds.[18] In 2009, our own group published the infected splinted mouse model, in which

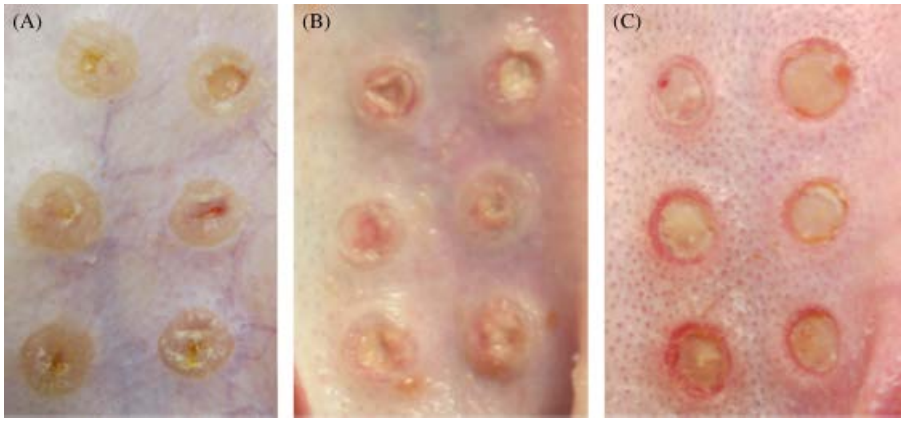

Figure 8. Photographs of control (uninfected) and infected wounds at POD 12. Control (A), active infection (B), and biofilm infection (C). Note the absence of purulence and debris in biofilm wounds as compared with active infection wounds, instead showing a ''film'' of bacteria spread across the wound. Also note the clear difference in extent of wound epithelialization between control and infected wounds. POD, postoperative day.

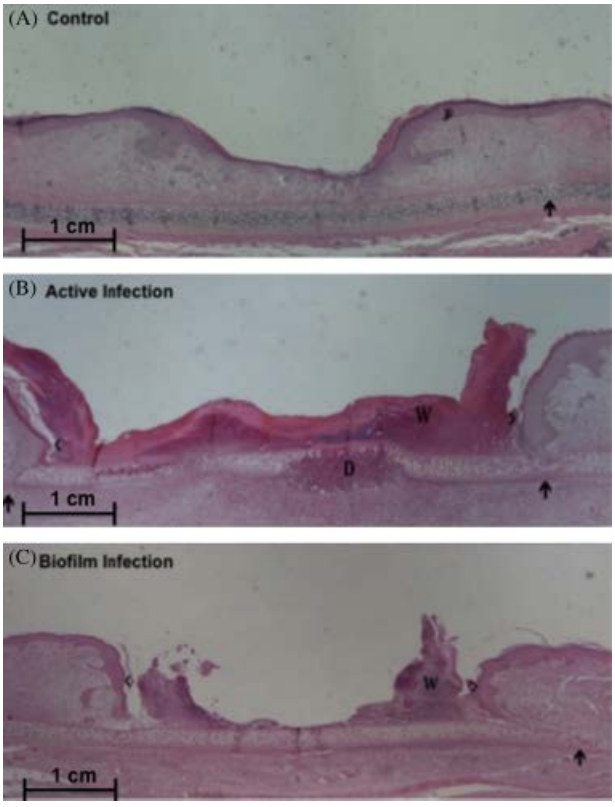

Figure 9. Wound healing histology. Hematoxylin & eosin staining of POD 12 rabbit ear wounds from control (A), active infection (B), and biofilm infection (C) groups. The wound edge was determined by the appearance of a nick in the cartilage made during wounding. Cartilage nick (arrow), epidermal thickening (arrow head), cartilage degradation (D), and debris from white blood cell influx (W) are labeled (magnification, ×20 [A–C]).POD, postoperative day.

open wounds were inoculated with either biofilm- or non-biofilm–forming bacteria, and treated with a biofilm inhibiting peptide; data from this paper suggested delayed epithelialization of these wounds, and that this delay was a biofilm-dependent effect.[19] Most recently Zhao et al.[20] have developed an infected wound model in db/db mice, applying preformed *P. aeruginosa* biofilm to full-thickness punch wounds, and found a marked reduction in a gross measure (percent healing) of infected vs. noninfected wounds.

Despite the advances in vivo animal modeling, currently available wound biofilm models possess certain limitations and shortcomings. In trying to address these deficiencies, we have developed the aforementioned rabbit ear wound biofilm model, which we believe is the most accurate representation of biofilm-infected human chronic wounds to date. Our model utilizes an adaptation of the rabbit dermal ulcer model,[21] an FDA-recognized model of wound healing that has been utilized by our lab and others for 20 years.[22–30] In this model, full-thickness, circular punch-wounds are made in the ears of New Zealand White rabbits down to cartilage, affording a number of important advantages. For example, in contrast to partial-thickness wounds, this removal of dermis more closely models the dermal-loss seen in human chronic wounds. Additionally, the majority of human wounds heal through epithelialization and granulation, in contrast to the contracture-based healing seen in mice.[19] The underlying cartilage of the rabbit ear serves as a natural splint, preventing healing by contracture, and thus allowing for accurate quantification of epithelial and granulation tissue formation from the periphery of the wound. Previous work with the rabbit ear dermal ulcer model has also showed that hypertrophic scarring within the rabbit ear is similar to that seen in humans grossly, histologically, and in its response to scar treatments such as steroid injection.[31,32] Moreover, multiple identical wounds can be made in one animal with contralateral controls, creating both a standardized and high-throughput wound model. Inoculation of wounds is done on postwounding day 3 using culture medium-grown bacteria with a measured size of inoculum of approximately 10^6 CFUs of bacteria. In contrast to other published models where preformed in vitro biofilm is directly applied to wounds, we believe that inoculation with planktonic, free-floating bacteria more closely represents the seeding mechanism of human chronic wounds, with the wound bed itself playing a critical role in the transformation of bacteria into the biofilm state.[33,34] Furthermore, as suggested by our presented data, inoculation in this manner triggers the formation of biofilm-phase bacteria within 24 hours.

In another significant departure from other published animal models, following in vivo proliferation of the inoculated bacteria, including formation of bacterial biofilm, our wounds are treated with topical antibiotic. As expected, this reduces the presence of active, planktonic-phase bacteria, but also by definition leaves behind what should be predominantly biofilm-phase bacteria, which are more resistant to antimicrobial challenge due to a protective ECM. We then utilize a combination of an occlusive dressing (Tegaderm®) with an underlying antimicrobial (polyhexamethylene biguanide) absorptive gauze pad (AMD Telfa®). This form of wound coverage helps maintain the predominance of biofilm-phase bacteria in two ways. First the antimicrobial impregnation of the gauze helps limit proliferation of planktonic bacteria. Second, it is clear that actively infected wounds are predisposed to the formation of purulent exudates. Previously published models have utilized fluid impermeable, occlusive dressings for their infected wounds without an underlying absorptive gauze pad.[19,20] Clinical observations, as well as our own pilot studies, demonstrate that placement of occlusive dressings over this developing fluid collection creates a seroma within the dead space beneath the dressing, representing an ideal culture medium for proliferation of planktonic-phase bacteria. In this setting a mixed planktonic-biofilm infection can become a predominantly planktonic, purulent infection, more similar to a superficial abscess than the wound surface biofilms seen in chronic wounds. Therefore, the use of absorptive gauze helps to minimize seroma formation, which when combined with previously administered antibiotics, creates a "steady-state" predominantly biofilm-phase infection by POD 6. Finally, we also perform frequent dressing changes before wound harvest, modeling the common clinical management of chronic wounds. In summary, our in vivo wound biofilm model is the most accurate and consistent

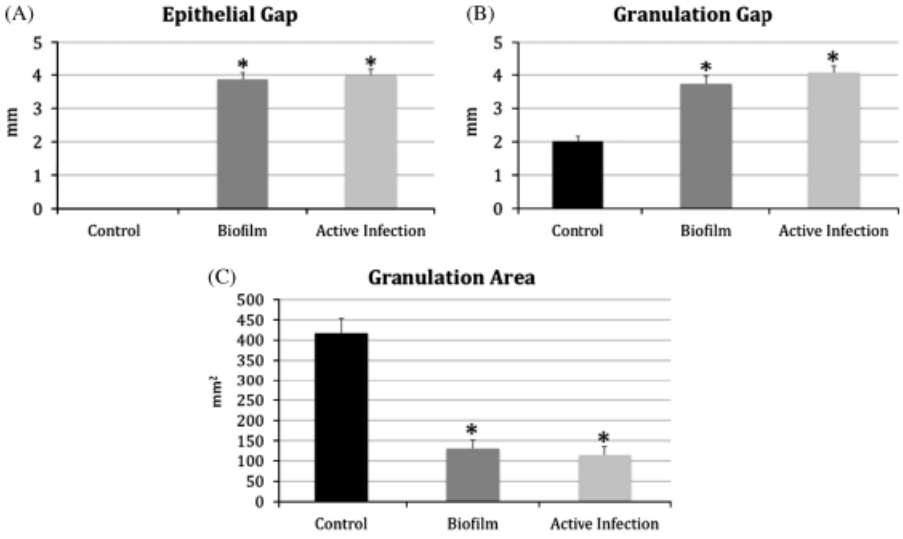

Figure 10. Quantification of healing parameters for uninfected (control), active-, and biofilm-infected wounds. (A) Epithelial gap, (B) granulation gap, and (C) granulation tissue area. Infected wounds have significantly less healing across all measured parameters when measure to control wounds, verifying in particular that biofilm does impair cutaneous wound healing and that this result is effectively simulated with this model (*$p < 0.05$ as compared with control wounds) (n=8–12 wounds/group). Error bars signify standard error of means.

simulation of biofilm-infected human chronic wounds to date, which we validate through the data presented in this manuscript.

Development of a model requires systemic testing and verification before it can be used for experimentation and analysis. We have presented an extensive set of data demonstrating this validation. Using epifluorescence and SEM, we have shown that inoculation with planktonic *S. aureus* establishes mature biofilm in cutaneous wounds, with marked speed and under no special conditions. To ensure that our model maintains viable biofilm-phase bacteria over the course of our protocol timeline, we measured viable bacterial counts at various time points postwounding and -inoculation. Although our development of a biofilm-predominant infection through antimicrobial techniques does decrease viable bacterial counts from their postinoculation values, the consistent level of bacteria seen between POD 6 and POD 12 reveals a trend that models the ''steady-state'' or chronic nature of biofilm, and directly correlates to the static nature of human chronic wounds. Corroborating this bacterial count analysis, we used laser scanning confocal microscopy and SEM to verify the physical presence of viable bacteria within the wound bed and the existence of complex biofilm structure morphologically at POD 12. These experiments clearly indicate that our model is capable of developing consistent wound biofilms that provide a foundation for further biofilm characterization and experimentation.

We then aimed to assess the capabilities and sensitivity of our model, utilizing quantitative analysis of host inflammatory gene expression to distinguish between our developed biofilm wounds and untreated, planktonic-dominant, active infection wounds. Correlating with clinical suspicion, we have shown that there is a distinct phenotypic difference between biofilm and active infection wounds. In particular, despite similar bacterial burdens, the host wound bed shows a unique inflammatory mediator profile in response to the biofilm phenotype. Additionally, we verified that this unique profile, characterized by a low-grade inflammatory response, is maintained over time within biofilm-infected wounds and that using our model it is localized to the wound bed, similar to a human chronic wound that elicits little systemic inflammatory effects. Taking the clinical applicability of our model further, we investigated the impairment of wound healing related to biofilm, an increasingly recognized phenomenon in nonhealing wounds. Grossly, there is a clear difference in both the host inflammatory response and extent of healing between infected and control wounds, which is further supported by histological analysis. In fact, quantitative analysis yields statistically significant differences in multiple histological wound healing parameters between uninfected and biofilm-infected wounds. Interestingly, vs. granulation tissue formation, we found maximal impairment to be in reepithelialization of biofilm-infected wounds. This observation agrees well with the frequent clinical observation of receding of epithelium or complete failure of reepithelialization (even in the face of adequate granulation tissue) in human wounds. These findings suggest that the primary mechanism of biofilm impairment of wound healing may be through inhibition of epithelialization. Although our data only represents part of the continued investigation into biofilm, we submit that our model provides a powerful in vivo methodology for wound biofilm study that is capable of quantitative, reproducible, and sensitive data analysis through both imaging and nonimaging modalities.

Although we have ensured biofilm phase infection and mirrored key inflammatory aspects of chronic wounds in this model, our assessment of wound healing is still occurring within an acute timeframe. Further work will be necessary to investigate the long-term effects of our biofilm protocol. Moreover, although morphology based on SEM is the current gold standard for identifying bacterial biofilms, it would have been ideal to confirm biofilm phenotype in more specific ways. Unfortunately, visualization by fluorescence is currently limited to using nonspecific carbohydrate markers as concanavalin A, as no specific markers for biofilm yet exist. In addition, our work thus far has been limited to a single species of bacteria, namely *S. aureus*. Organisms such as *P. aeruginosa* and various anaerobic bacteria are also very common within chronic

wound microbial flora. With work currently under way, it will be useful to extend our investigation to other bacterial species, furthering our understanding of the model's capabilities and shortcomings.

Despite these limitations, we believe the rabbit biofilm model to have considerable strengths. As described, our model has been adapted from an FDA-recognized rabbit dermal ulcer model, which provides a robust ability to quantify wound healing through multiple measures of epithelialization and granulation tissue formation. Data can also be obtained in a relatively high-throughput manner, with as many as 12 wounds per animal. The rabbit model is also highly versatile, existing in various ischemic, venous stasis, reperfusion injury, and diabetic iterations.[21,35] In addition, we have developed our model taking into account both the defining characteristics of human chronic wounds as well as the limitations posed by other current in vitro and in vivo biofilm models. Having an in vivo platform allows us to model the bacterial–host interaction, which is lost through in vitro analysis, with a high level of sensitivity. The reproducibility and precision of the model also allows for systematic analysis of wound healing changes secondary to bacterial manipulation or wound treatment, creating an ideal model for the testing of antibiofilm therapeutics.

With the establishment of validated in vivo biofilm model, we now have a foundation for exploring several interesting and significant avenues of investigation. In particular, what is the clinically relevant level of biofilm burden that prevents wound healing? Do some strains of bacteria inhibit wound healing to a greater extent than others? What is the mechanism of bacterial impairment of wound healing? What is the effect of polybacterial infections on wound healing? Lastly, what are the ideal treatments and treatment regimens against wound biofilms that will promote healing? It is our hope that now equipped with sufficiently validated and complementary in vitro and in vivo biofilm models, we can begin making strides in our understanding of the basic biology of bacterial wound biofilms, and move ever closer toward the successful treatment of human chronic wounds.

ACKNOWLEDGMENTS

The NRS623 was obtained through the Network of Antimicrobial Resistance in *S. aureus* (NARSA) program supported under NIAID/NIH Contract # HHSN 272200700055C.

REFERENCES

1. Hall Stoodley L, Costerton JW, Stoodley P. Bacterial bio films: from the natural environment to infectious diseases. *Nat Rev Microbiol* 2004; 2: 95 108.
2. Parsek MR, Singh PK. Bacterial biofilms: an emerging link to disease pathogenesis. *Annu Rev Microbiol* 2003; 57: 677 701.
3. James GA, Swogger E, Wolcott R, Pulcini E, Secor P, Sest rich J, Costerton JW, Stewart PS. Biofilms in chronic wounds. *Wound Repair Regen* 2008; 16: 37 44.
4. Gjodsbol K, Christensen JJ, Karlsmark T, Jorgensen B, Klein BM, Krogfelt KA. Multiple bacterial species reside in chronic wounds: a longitudinal study. *Int Wound J* 2006; 3: 225 31.
5. Bjarnsholt T, Kirketerp Moller K, nsen PØ, Madsen KG, Phipps R, Krogfelt K, Høiby N, Givskov M. Why chronic wounds will not heal: a novel hypothesis. *Wound Repair Re gen* 2008; 16: 2 10.
6. Anderson GG, O'Toole GA. Innate and induced resistance mechanisms of bacterial biofilms. *Curr Top Microbiol Im munol* 2008; 322: 85 105.
7. Kong KF, Vuong C, Otto M. Staphylococcus quorum sens ing in biofilm formation and infection. *Int J Med Microbiol* 2006; 296: 133 9.
8. Kirker KR, Secor PR, James GA, Fleckman P, Olerud JE, Stewart PS. Loss of viability and induction of apoptosis in human keratinocytes exposed to *Staphylococcus aureus* bio films in vitro. *Wound Repair Regen* 2009; 17: 690 9.
9. Blevins JS, Elasri MO, Allmendinger SD, Beenken KE, Skin ner RA, Thomas JR, Smeltzer MS. Role of sarA in the pathogenesis of *Staphylococcus aureus* musculoskeletal infec tion. *Infect Immun* 2003; 71: 516 23.
10. Beenken KE, Dunman PM, McAleese F, Macapagal D, Murphy E, Projan SJ, Blevins JS, Smeltzer MS. Global gene expression in *Staphylococcus aureus* biofilms. *J Bacteriol* 2004; 186: 4665 84.
11. Charpentier E, Anton AI, Barry P, Alfonso B, Fang Y, Novick RP. Novel cassette based shuttle vector system for gram posi tive bacteria. *Appl Environ Microbiol* 2004; 70: 6076 85.
12. Zhao LL, Davidson JD, Wee SC, Roth SI, Mustoe TA. Effect of hyperbaric oxygen and growth factors on rabbit ear ischemic ulcers. *Arch Surg* 1994; 129: 1043 9.
13. Menke NB, Ward KR, Witten TM, Bonchev DG, Diegel mann RF. Impaired wound healing. *Clin Dermatol* 2007; 25: 19 25.
14. Wolcott RD, Rhoads DD, Bennett ME, Wolcott BM, Gogokhia L, Costerton JW, Dowd SE Chronic wounds and the medical biofilm paradigm. *J Wound Care* 2010; 19: 45 6, 48 50, 52 3.
15. Mustoe TA, O'Shaughnessy K, Kloeters O. Chronic wound pathogenesis and current treatment strategies: a unifying hy pothesis. *Plast Reconstr Surg* 2006; 117 (Suppl.): 35S 41S.
16. Edwards R, Harding KG. Bacteria and wound healing. *Curr Opin Infect Dis* 2004; 17: 91 6.
17. Rashid MH, Rumbaugh K, Passador L, Davies DG, Ha mood AN, Iglewski BH, Kornberg A. Polyphosphate kinase is essential for biofilm development, quorum sensing, and virulence of *Pseudomonas aeruginosa*. *Proc Natl Acad Sci USA* 2000; 97: 9636 41.
18. Davis SC, Ricotti C, Cazzaniga A, Welsh E, Eaglstein WH, Mertz PM. Microscopic and physiologic evidence for bio film associated wound colonization in vivo. *Wound Repair Regen* 2008; 16: 23 9.
19. Schierle CF, De la Garza M, Mustoe TA, Galiano RD. Staphylococcal biofilms impair wound healing by delaying reepithelialization in a murine cutaneous wound model. *Wound Repair Regen* 2009; 17: 354 9.
20. Zhao G, Hochwalt PC, Usui ML, Underwood RA, Singh PK, James GA, Stewart PS, Fleckman P, Olerud JE. Delayed wound healing in diabetic (db/db) mice with *Pseudomonas aeruginosa* biofilm challenge: a model for the study of chronic wounds. *Wound Repair Regen* 2010; 18: 467 77, Epub Au gust 19, 2010.
21. Ahn ST, Mustoe TA. Effects of ischemia on ulcer wound healing: a new model in the rabbit ear. *Ann Plast Surg* 1990; 24: 17 23.

22. Mogford JE, Tawil B, Jia S, Mustoe TA. Fibrin sealant com bined with fibroblasts and platelet derived growth factor en hance wound healing in excisional wounds. *Wound Repair Regen* 2009; 17: 405 10.
23. Mustoe TA, Pierce GF, Morishima C, Deuel TF. Growth factor induced acceleration of tissue repair through direct and inductive activities in a rabbit dermal ulcer model. *J Clin Invest* 1991; 87: 694 703.
24. Mustoe TA, Tae Ahn S, Tarpley JE, Pierce GF. Role of hypo xia in growth factor responses: differential effects of basic fibro blast growth factor and platelet derived growth factor in an ischemic wound model. *Wound Repair Regen* 1994; 2: 277 83.
25. Galiano RD, Zhao LL, Clemmons DR, Roth SI, Lin X, Mustoe TA. Interaction between the insulin like growth fac tor family and the integrin receptor family in tissue repair processes. Evidence in a rabbit ear dermal ulcer model. *J Clin Invest* 1996; 98: 2462 8.
26. Wu L, Xia YP, Roth SI, Gruskin E, Mustoe TA. Transform ing growth factor beta1 fails to stimulate wound healing and impairs its signal transduction in an aged ischemic ulcer model: importance of oxygen and age. *Am J Pathol* 1999; 154: 301 9.
27. Chen EA, Zhao L, Bamat M, von Borstel R, Mustoe T. Ac celeration of wound healing with topically applied deoxyri bonucleosides. *Arch Surg* 1999; 134: 520 5.
28. Xia YP, Zhao Y, Marcus J, Jimenez PA, Ruben SM, Moore PA, Khan F, Mustoe TA. Effects of keratinocyte growth fac tor 2 (KGF 2) on wound healing in an ischaemia impaired rabbit ear model and on scar formation. *J Pathol* 1999; 188: 431 8.
29. Lu L, Saulis AS, Liu WR, Roy NK, Chao JD, Ledbetter S, Mustoe TA. The temporal effects of anti TGF beta1, 2, and 3 monoclonal antibody on wound healing and hypertrophic scar formation. *J Am Coll Surg* 2005; 201: 391 7.
30. Said HK, Hijjawi J, Roy N, Mogford J, Mustoe T. Trans dermal sustained delivery oxygen improves epithelial healing in a rabbit ear wound model. *Arch Surg* 2005; 140: 998 1004.
31. Sisco M, Kryger ZB, O'Shaughnessy KD, Kim PS, Schultz GS, Ding XZ, Roy NK, Dean NM, Mustoe TA. Antisense inhibition of connective tissue growth factor (CTGF/CCN2) mRNA limits hypertrophic scarring without affecting wound healing in vivo. *Wound Repair Regen* 2008; 16: 661 73.
32. Kloeters O, Tandara A, Mustoe TA. Hypertrophic scar model in the rabbit ear: a reproducible model for studying scar tissue behavior with new observations on silicone gel sheeting for scar reduction. *Wound Repair Regen* 2007; 15: S40 5.
33. Schultz GS, Barillo DJ, Mozingo DW, Chin GA, Wound Bed Advisory Board Members. Wound bed preparation and a brief history of TIME. *Int Wound J* 2004; 1: 19 32.
34. Cierny G III, DiPasquale D. Treatment of chronic infection. *J Am Acad Orthop Surg* 2006; 14: S105 10.
35. Breen A, Mc Redmond G, Dockery P, O'Brien T, Pandit A. Assessment of wound healing in the alloxan induced diabetic rabbit ear model. *J Invest Surg* 2008; 21: 261 9.